INFLUENCE OF END GEOMETRY ON FIBER REINFORCED ELASTOMERIC ISOLATOR BEARINGS

M. J. Tait [1], H. Toopchi-Nezhad [2], and R. G. Drysdale [3]

[1] *Assistant Professor, Dept. of Civil Engineering , McMaster University, Hamilton, Canada*
[2] *Ph.D. Candidate, Dept. of Civil Engineering , McMaster University, Hamilton, Canada*
[3] *Professor Emeritus, Dept. of Civil Engineering , McMaster University, Hamilton, Canada*
Email: taitm@mcmaster.ca, toopchh@mcmaster.ca, drysdale@mcmaster.ca

ABSTRACT :

The isolators investigated in this paper comprise a novel base isolation system developed specifically for the seismic mitigation of ordinary low-rise buildings. This novel base isolation system employs “Stable Unbonded Fiber Reinforced Elastomeric Isolators” (SU-FREI). A fiber reinforced elastomeric isolator utilizes fiber fabric, such as carbon fiber, as the reinforcement material instead of solid steel plates. The fiber fabric reinforcement is extensible in tension and has no flexural rigidity. In an unbonded application, the FREI bearings are placed between the superstructure and substructure with no bonding or fastening required between the contact surfaces. An experimental study is conducted on model scale prototype FREI bearings constructed using unfilled soft Neoprene rubber as the elastomer, and bi-directional carbon fiber fabric as the reinforcement. Three different end geometries are considered and the influence of the different end configurations on the response behavior of the isolators is investigated by means of cyclic testing.

KEYWORDS: stable unbonded fiber reinforced elastomeric isolator (SU-FREI), end geometry, stable rollover, unbonded application, laminated rubber bearing

1. INTRODUCTION

Steel-Reinforced Elastomeric Isolator (SREI) bearings are the most common type of isolator in use but because of their size, weight and cost applications are primarily justified only for large and expensive buildings and have not been extended to ordinary housing and commercial buildings. The heavy weight is due to the steel reinforcing plates. The high cost is primarily due to the labor-intensive manufacturing process and vulcanization, which occurs under high pressure and temperature (Kelly 2002). However, potential cost savings exist if the steel reinforcing plates are replaced with other materials having approximately the same elastic modulus as steel, so that the manufacturing process of the isolator becomes easier and less labor-intensive.

Fiber-Reinforced Elastomeric Isolator (FREI) bearings are a relatively new type of laminated bearing, which utilizes carbon fiber fabric as the reinforcement to reduce lateral bulging and to develop the required level of vertical stiffness. Initial studies (Kelly 1999) have indicated that FREI bearings can achieve adequate values of vertical and horizontal stiffness. Furthermore, FREI bearings have a number of advantages over SREI bearings including superior energy dissipation capability, potential low manufacturing cost, light-weight, and the prospect of being produced in long rectangular strips and modified to the required size locally.

A distinct type of FREI bearing, designated as a Stable Unbonded Fiber Reinforced Elastomeric Isolator (SU-FREI) bearing, is placed between the superstructure and foundation; however there is no bonding or fastening between the isolator and the contact surfaces as is required in the traditional installation of bearings. As a result of using a reinforcing material with no bending stiffness and an unbonded installation technique, an SU-FREI bearing has a unique Stable Rollover (SR) deformation characteristic. This SR characteristic has been found to improve the effectiveness of this seismic isolation device (Toopchi-Nezhad et al. 2007 and 2008).

This paper presents the results of a preliminary experimental study conducted to investigate the influence of end geometry on the response behavior of SU-FREI bearings. Four SU-FREI bearings with different end geometries are experimentally investigated and the results are compared to evaluate the influence of this parameter on the lateral force-displacement properties of SU-FREI bearings.

2. MODIFICATIONS TO SURROUNDING CONTACT SURFACES AND VERTICAL BEARING FACES

Due to the unbonded application technique and fiber fabric reinforcement employed by SU-FREI bearings, they deform significantly differently than traditional bearings when subject to lateral deflections. This is illustrated in Figure 1, which compares the deformation pattern of a bearing having rigid plates bonded at its bearing surfaces to that of a SU-FREI bearing. It is evident from Figure 1 that the unbounded application permits the contact boundary surfaces of the SU-FREI bearing to change as the bearing is displaced laterally. As a result, a new parameter, namely the geometry of the contact surfaces, can be modified to alter the response behavior of the bearings.

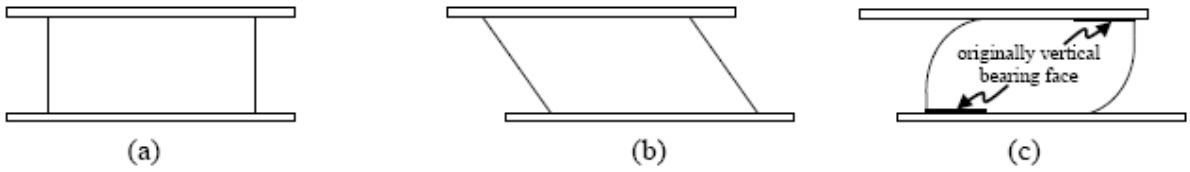

Figure 1. (a) Undeformed bearing (b) deformation pattern for a typical bearing (bonded) and (c) deformation pattern for a SU-FREI (unbonded).

Figure 2 shows several examples of different modifications that can be made to the vertical faces of the bearing

itself or the surrounding contact surfaces in order to alter the response behavior of an SU-FREI bearing. Changes to the surrounding contact surfaces and vertical faces of the bearing will influence the horizontal force that develops as the bearing is displaced laterally. These proposed modifications are expected to accelerate, delay or modify the stiffening effect leading to stable rollover.

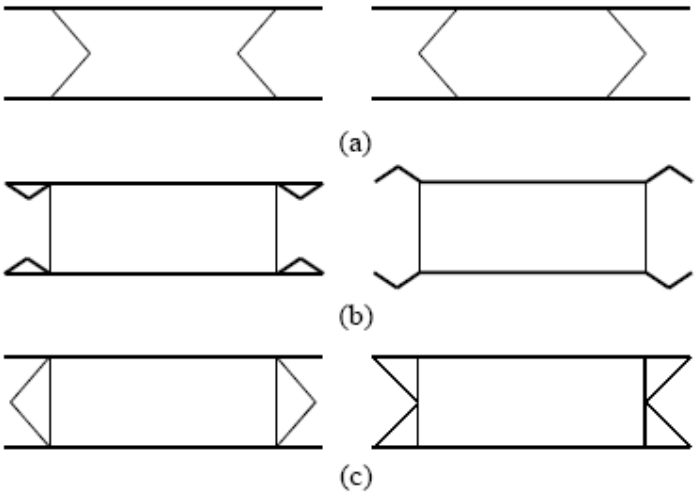

Figure 2. Examples of (a) modified shape of vertical faces of bearing (b) modified shape of surrounding contact surface and (c) preformed shapes fastened to vertical faces of bearing.

2.1. Modified Vertical Bearing Faces – End Geometries

The illustrations and photograph in Figure 3 show the four SU-FREI bearings investigated in this study.

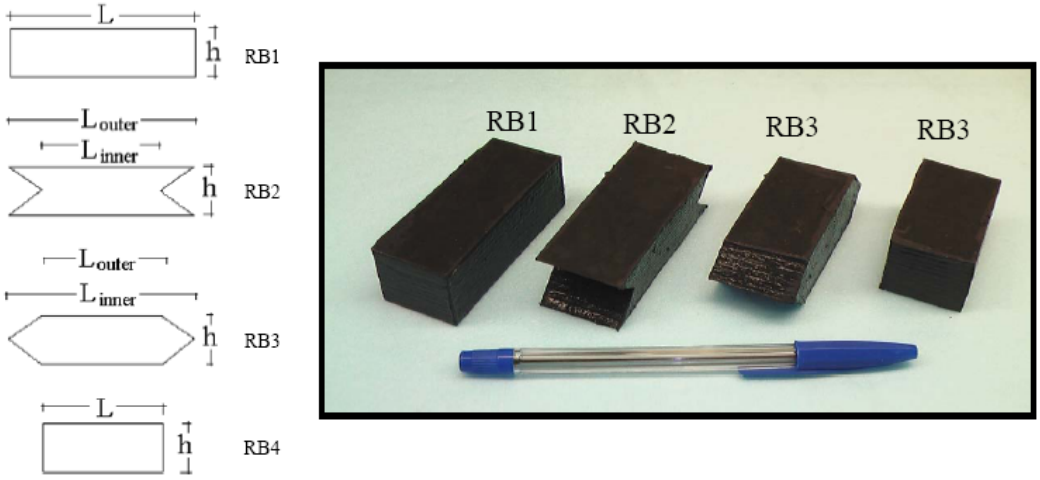

Figure 3. Illustrations and photograph of FREI bearings with different end geometries.

The bearing dimensions are listed in Table 2.1. The width, b, of all four bearings was held constant. Two rectangular bearings with vertical end geometry, RB1 and RB4, were selected in order to bracket the expected aspect ratio, R, and shape factor, S, values for bearings RB2 and RB3. The shape factor controls the effective compression modulus of the rubber-reinforcement composite under a specified level of vertical load and the aspect ratio affects bearing stability (Kelly 1997). Additionally, the aspect ratio is a key parameter in achieving

Stable Rollover deformation in SU-FREI bearings (Toopchi-Nezhad et al. 2007).

Table 2.1 Nominal bearing dimensions

Bearing	b (mm)	h (mm)	L (mm)		R (aspect ratio)	S (shape factor)
			L_{inner}	L_{outer}		
RB1	31	24	76		3.2	6.9
RB2	31	23	52	74	2.2-3.2	6.1-6.9
RB3	31	23	74	52	2.2-3.2	6.1-6.9
RB4	31	24	52		2.2	6.1

2.2. Experimental Setup

Cyclic tests were conducted on the bearings to determine their horizontal stiffness values and damping values as well as to verify their suitability as seismic isolation devices in an unbonded application. A photograph of the test apparatus is shown in Figure 4a. In order to properly simulate the boundary conditions, the bearings were not bonded to the platens of the test apparatus for the cyclic load testing. The cyclic tests were carried out using displacement control in the horizontal direction to apply the lateral motions and load control in the vertical direction to maintain a constant vertical load during application of the lateral displacement time history shown in Figure 4b.

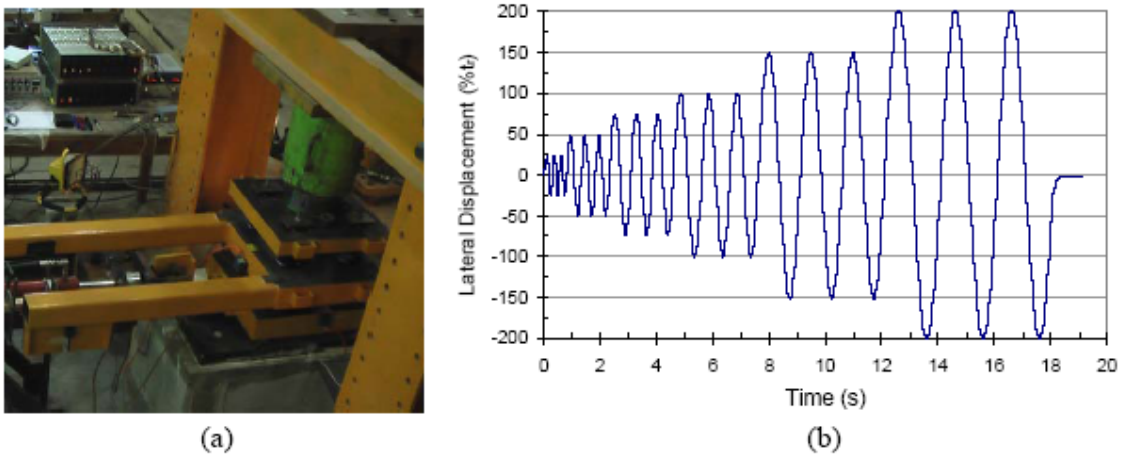

Figure 4. (a) Photograph of the test apparatus and (b) time history of input lateral displacements.

As observed from Figure 4b, each bearing was subjected to a total of 18 displacement cycles consisting of three cycles at six different amplitudes. The relative horizontal movement between the platens was measured using a string pot and the horizontal forces were measured by a load cell. Four laser displacement transducers were used to measure the vertical deflection of the bearing at its four sides and four identical and symmetrically placed load cells were used to measure the vertical load. A more detailed description of the experimental setup and test apparatus can be found elsewhere (Toopchi-Nezhad et al. 2007).

3. CYCLIC TEST RESULTS

Rollover deformation results from a lack of flexural rigidity in the fiber reinforcement layers and the unbonded boundary condition of the bearing at its contact surfaces. This results in a significant reduction in the horizontal stiffness of the bearing, which is considered acceptable if the resulting incremental lateral load-resisting capacity of the bearing remains positive. In addition, when the vertical faces of the bearing touch the upper and lower platens at the extreme lateral displacements, a hardening type behavior is observed. This hardening behavior (increased stiffness) limits the maximum lateral displacement of the bearing, thus ensuring the bearing remains stable at the maximum considered earthquake. As such, this rollover deformation is called Stable Rollover (SR). It should be noted that SR deformation does not introduce a negative lateral load-resisting capacity nor does it compromise the overall stability of the bearing. It does, however, add to the efficiency of the bearing as the horizontal stiffness is reduced and, as a result, this unique characteristic is considered advantageous for application of FREIs with unbonded contact surfaces.

Photographs of all four bearings at lateral displacement amplitudes of 0%, 100% and 200% of the total thickness of rubber layers, t_r, are shown in Figure 5. It can be observed from Figure 5 that at extreme lateral displacements, i.e. 200% t_r the total contact area between the end faces of the bearing and the upper and lower platens are influenced by bearing end geometry. The end geometry of an SU-FREI bearing also influences the amplitude at which the end faces of the bearing first make contact with the upper and lower platens and the deformed shape of the bearing when subject to lateral displacements.

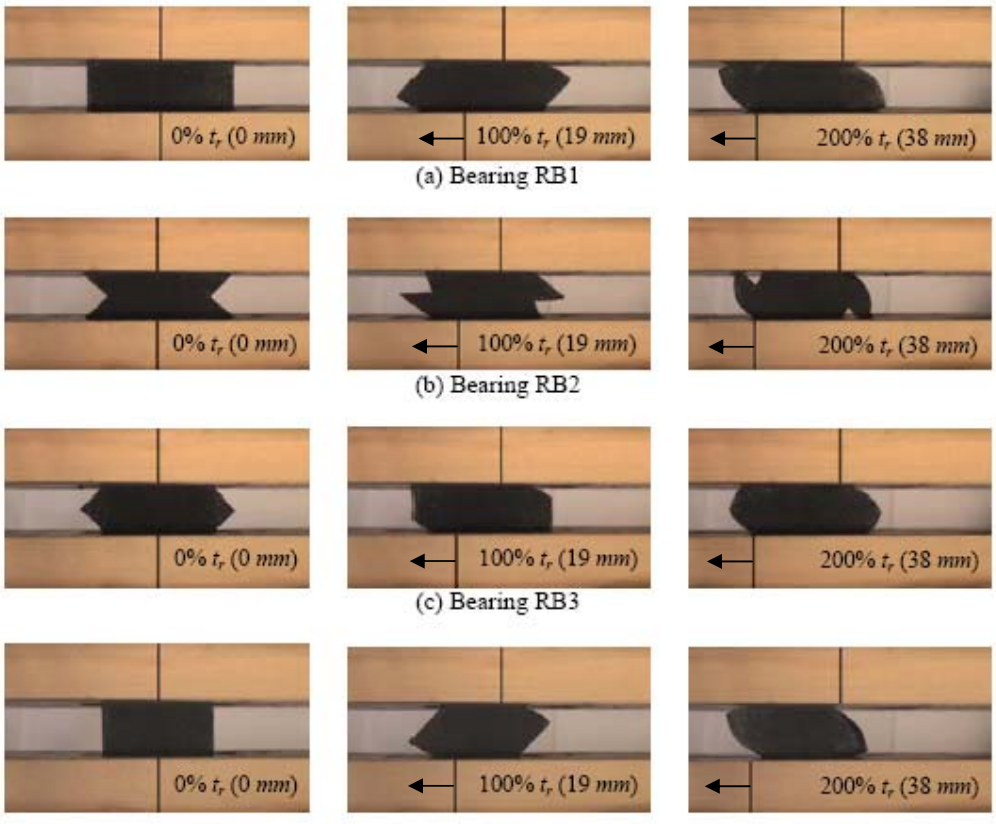

Figure 5. Photographs of the of SU-FREI bearings (a) RB1, (b) RB2, (c) RB3 and (d) RB4 at different lateral displacement amplitudes during cyclic testing.

3.1. Hysteretic Behavior

Plots of the horizontal force-displacement hysteresis loops for all four bearings are shown in Figure 6. Inspection of the hysteresis loops indicates that the bearings tested; 1) maintained positive incremental load-resisting capacity; 2) exhibited a softening type behavior (decreased stiffness) due to rollover deformation; and 3) exhibited a hardening type behavior (increased stiffness) at large lateral displacement amplitudes. Therefore, all four bearings satisfy SU-FREI criteria (Toopchi-Nezhad et al. 2007).

RB2 and RB3 can be considered as modified versions of bearings RB1 and RB4. By removing material from the end faces of RB1 or adding material to the end faces of RB4 bearings similar to RB2 and RB3 can be produced. Inspection of the hysteresis plots reveals that, compared to RB1, removing material from the end faces of the bearing leads to a reduction in the bearing stiffness, with the largest reduction in stiffness occurring in bearing RB3 at intermediate lateral displacement amplitudes. Compared to RB4, adding material to the end faces resulted in increased bearing stiffness.

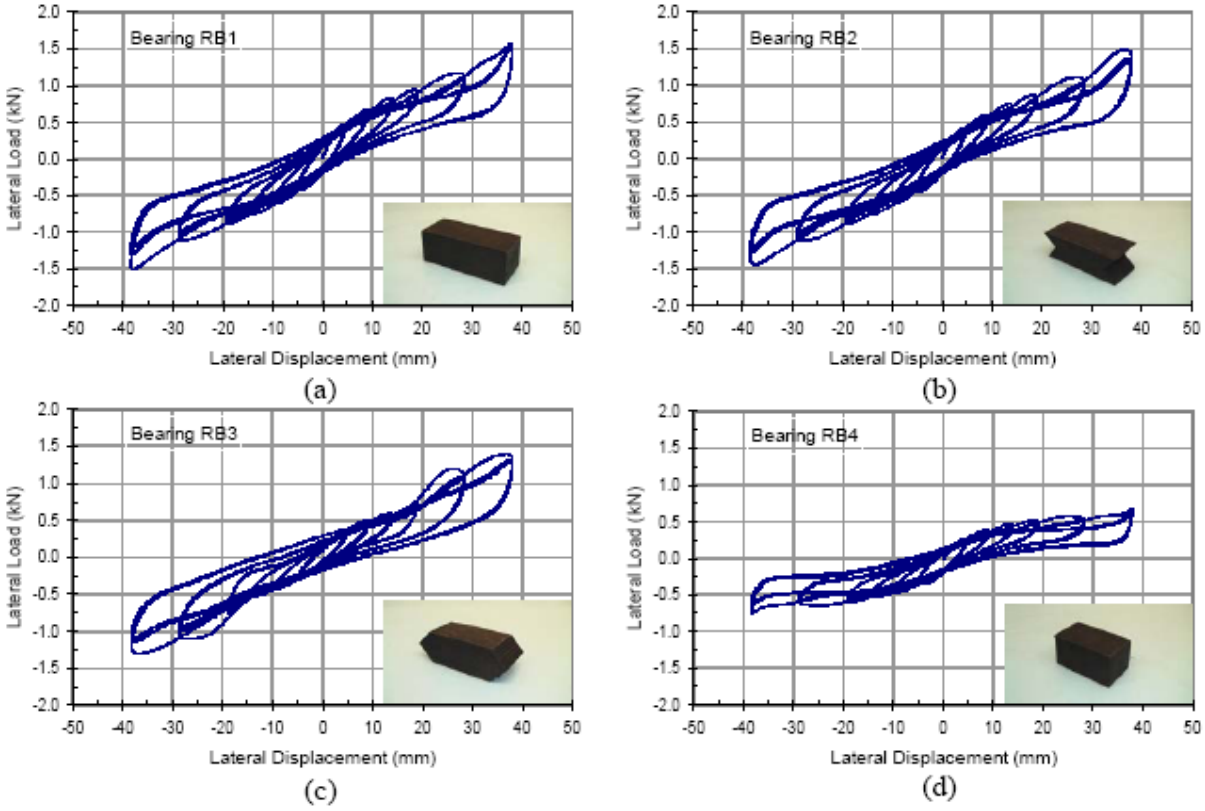

Figure 6. Horizontal force-displacement hysteretic loops for bearing (a) RB1, (b) RB2, (c) RB3 and (d) RB4 from cyclic test results.

4. EFFECTIVE HORIZONTAL STIFFNESS AND EQUIVALENT VISCOUS DAMPING

In order to make quantitative comparisons, the effective horizontal stiffness, K, of each bearing corresponding to each load cycle of the test, was calculated based on the peak lateral force and peak displacement (ASCE, 2005).

$$K = \frac{F_{max} - F_{min}}{\Delta_{max} - \Delta_{min}} \quad (4.1)$$

where F_{max}, F_{min}, Δ_{max} and Δ_{min} are the maximum and minimum values of horizontal force and horizontal displacement, respectively. The ratio of equivalent viscous damping, ξ, of each bearing was also determined by (Clough and Penzien 1975)

$$\xi = \frac{W_d}{4\pi W_s} \quad (4.2)$$

W_d is the dissipated energy per cycle and W_s is the elastic energy. W_s can be expressed as

$$W_s = \frac{K\,\Delta^2}{2} \quad (4.3)$$

where

$$\Delta = \frac{\Delta_{max} - \Delta_{min}}{2} \quad (4.4)$$

Table 4.1 Mechanical properties of the model scale FREI bearings

Displacement	Cycles	RB1		RB2		RB3		RB4	
		K (N/mm)	ξ (%)	K (N/mm)	ξ (%)	K (N/mm)	ξ (%)	K (N/mm)	ξ (%)
25% t_r (4.8 mm)	1	95.7	18.8	90.0	20.4	64.1	16.3	66.1	21.7
	2	88.8	20.3	84.1	23.2	61.5	14.8	61.6	23.3
	3	87.7	20.2	82.9	21.5	61.2	14.8	60.5	22.7
50% t_r (9.5 mm)	1	67.6	14.3	63.6	14.6	49.1	14.6	45.0	15.5
	2	62.8	13.3	59.2	13.3	45.3	13.7	41.2	14.5
	3	61.8	13.3	58.0	13.4	44.4	13.6	40.5	14.5
75% t_r (14.3 mm)	1	55.3	11.9	52.8	11.7	39.3	13.2	35.3	13.0
	2	51.7	11.4	49.0	11.3	36.5	12.8	32.3	12.7
	3	50.6	11.3	48.1	11.2	35.8	12.8	31.7	12.9
100% t_r (19.0 mm)	1	47.5	10.9	46.3	10.7	40.0	11.0	29.1	12.3
	2	44.8	10.3	43.2	10.1	38.4	10.5	27.0	12.0
	3	43.9	10.3	42.5	10.1	37.7	10.4	26.3	12.1
150% t_r (28.5 mm)	1	39.9	11	38.9	10.9	40.2	11.7	21.4	13.5
	2	37.3	9.7	36.0	9.8	36.5	10.5	19.1	13.0
	3	36.4	9.7	35.1	9.6	35.3	10.4	18.6	13.1
200% t_r (38.0 mm)	1	40.5	10	38.4	10.4	35.4	12.3	18.5	13.6
	2	37.2	9.1	34.7	9.5	32.3	11.9	17.2	13.0
	3	35.6	9.2	33.4	9.4	31.1	14.4	16.6	13.2

Results in Table 2 show bearings RB1 and RB2 had similar effective horizontal stiffness values over the range of lateral displacement amplitudes tested. The maximum difference between K values of RB1 and RB2 was found to be less than 7%. However, the effective horizontal stiffness of bearing RB3 was approximately 30% less than the effective horizontal stiffness of bearing RB1 for displacements of 75% t_r or less. Interestingly, due to the change in the force-displacement behavior, which can be observed in Figure 6, the K values for bearings RB1, RB2 and RB3 were approximately equal at 150% t_r. At 100% t_r and 200% t_r the effective horizontal stiffness of RB3 was approximately 10-15% less than RB1. Bearings RB1 and RB2 had similar equivalent viscous damping values over the range of lateral displacement amplitudes investigated. The equivalent viscous damping for RB3 was found to be less than RB1 at 25% t_r and gradually changed to be greater than RB1 at 200% t_r.

The effective stiffness values for bearing RB2 were found to be significantly larger than the values calculated for RB4 over the entire range of lateral displacement amplitudes. The effective horizontal stiffness of bearing

RB2 was approximately 40% greater than RB4 at 25% t_r and was found to have twice the effective horizontal stiffness at the largest lateral displacement amplitude. The effective horizontal stiffness of RB3 was approximately equal to RB4 at 25% t_r, however, the effective horizontal stiffness was found to increase relative to RB4 as the lateral displacement amplitude was increased. At 200% t_r displacement, the effective horizontal stiffness of RB3 was 1.9 times larger than RB4. The equivalent viscous damping values for RB2 and RB4 were approximately equal at 25% t_r. As the lateral displacement amplitude was increased, RB2 ξ values decreased relative to RB4 ξ values. Conversely, the equivalent viscous damping of RB3 was approximately 30% less than that of RB4 at 25% t_r and approximately equal at 200% t_r. These preliminary results indicate that end geometry influences both the effective lateral stiffness and the equivalent viscous damping of a SU-FREI bearing.

5. CONCLUSIONS

This paper has introduced the concept of modifying the end geometry of SU-FREI bearings. Four SU-FREI bearings with different end geometries were investigated. Two bearings were constructed with vertical end faces and had shape factor and aspect ratio values that bracketed the bearings with modified end geometries. Cyclic horizontal tests were performed on all four bearings. A comparison of the lateral force-displacement hysteresis loops showed that end geometry can significantly modify the lateral force-displacement response behavior of an SU-FREI bearing. The lateral stiffness of an SU-FREI bearing was found to decrease if material was removed from the end faces of the bearing and to increase if material was added to the end faces of the bearing. Additionally, the shape of the end face was found to affect the response behavior of the bearing. In addition to affecting the effective horizontal stiffness, modifying the end geometry of an SU-FREI bearing also has an influence on the equivalent viscous damping. These preliminary findings indicate that the end geometry of an SU-FREI bearing is a parameter that can be modified to obtain the desired lateral force-displacement response behavior. Additional studies are needed to determine optimal end geometries that maximize the seismic mitigation efficiency of SU-FREI bearings.

ACKNOWLEDGMENTS

This research was carried out as part of the mandate of the McMaster University Centre for Effective Design of Structures funded through Ontario Research and Development Challenge Fund (ORDCF). The authors also would like to gratefully acknowledge additional funding from the Ministry of Science, Research and Technology of Iran and the Natural Sciences and Engineering Research Council of Canada (NSERC).

REFERENCES

ASCE. (2005). Minimum Design Loads for Buildings and Other Structures, American Society of Civil Engineers, ASCE/SEI 7-05.
Clough, R., and Penzien, J., 1975. Dynamics of Structures, McGraw-Hill, New York.
Kelly, J.M. (1997). Earthquake Resistant Design with Rubber, 2nd edition, Springer-Verlag Berlin Heidelberg New York.
Kelly, J. M. (1999). Analysis of Fiber-Reinforced Elastomeric Isolators, Journal of seismology and earthquake engineering (JSEE), 2 (1), 19-34.
Kelly, J.M. (2002). Seismic Isolation Systems for Developing Countries, Earthquake Spectra, 18:3, 385-406.
Toopchi-Nezhad H., Tait M.J., and Drysdale R.G. (2007). Testing and modeling of square carbon fiber reinforced elastomeric seismic isolators. Journal of Structural Control and Health Monitoring, DOI: 10.1002/stc.225.
Toopchi-Nezhad H., Tait M.J., and Drysdale R.G. (2008). Lateral Response Evaluation of Fiber Reinforced Neoprene Seismic Isolators Utilized in an Unbonded Application. Structural Journal, ASCE, 134:10.